

1/19/96

ANL/PHY/CP-89168
CONF-960276--1

THE INTERACTIONS OF HIGH-ENERGY, HIGHLY-CHARGED IONS WITH FULLERENES

R. Ali*, H. G. Berry[†], S. Cheng[‡], R. W. Dunford, H. Esbensen, D. S. Gemmell, E. P. Kanter, T. LeBrun, and L. Young

Physics Division, Argonne National Laboratory, Argonne, Illinois 60439

W. Bauer

NSCL, Michigan State University, East Lansing, Michigan 48824

In 1985, Robert Curl and Richard Smalley¹ discovered a new form of carbon, the fullerene, C₆₀, which consists of 60 carbon atoms in a closed cage resembling a soccer ball. In 1990, Krätschmer et al. were able to make macroscopic quantities of fullerenes². This has generated intense activity to study the properties of fullerenes. One area of research involves collisions between fullerenes and atoms, ions or electrons^{3,4}. In this paper we describe experiments involving interactions between fullerenes and highly charged ions in which the center-of-mass energies exceed those used in other work by several orders of magnitude. The high values of projectile velocity and charge state result in excitation and decay processes differing significantly from those seen in studies at lower energies³. Our results are discussed in terms of theoretical models analogous to those used in nuclear physics and this provides an interesting demonstration of the unity of physics.

In our experiments, 420-625 MeV beams of ¹³⁶Xe³⁵⁺ or ¹³⁶Xe¹⁸⁺ ions from Argonne's ATLAS accelerator were incident on a C₆₀ vapor target formed from 99.5% pure C₆₀ heated to 475 °C in a two-stage stainless-steel oven. The target had a density of $\sim 10^{10}$ molecules/cm³ in the interaction region. A time-of-flight (TOF) spectrometer system was located at 90° to the ion beam. Grids around the target region were biased with voltages to extract positively charged fragments. The fragments passed through a 20-cm-long gridded flight tube to a micro-channel-plate detector. The total acceleration voltage was 6.9 kV. A "beam sweeper" allowed one 0.4 ns-wide beam pulse to reach the target every 10 μ s. TOF spectra were obtained using a "multi-hit" time digitizer with the "start" signal coming from the detector and the "stop" signal from

*Present address: Department of Physics, University of Nevada, Reno, Nevada 89557.

[†]Department of Physics, University of Notre Dame, Notre Dame, Indiana 46556.

[‡]Present address: Department of Physics, University of Toledo, Toledo, Ohio 43606.

DISCLAIMER

**Portions of this document may be illegible
in electronic image products. Images are
produced from the best available original
document.**

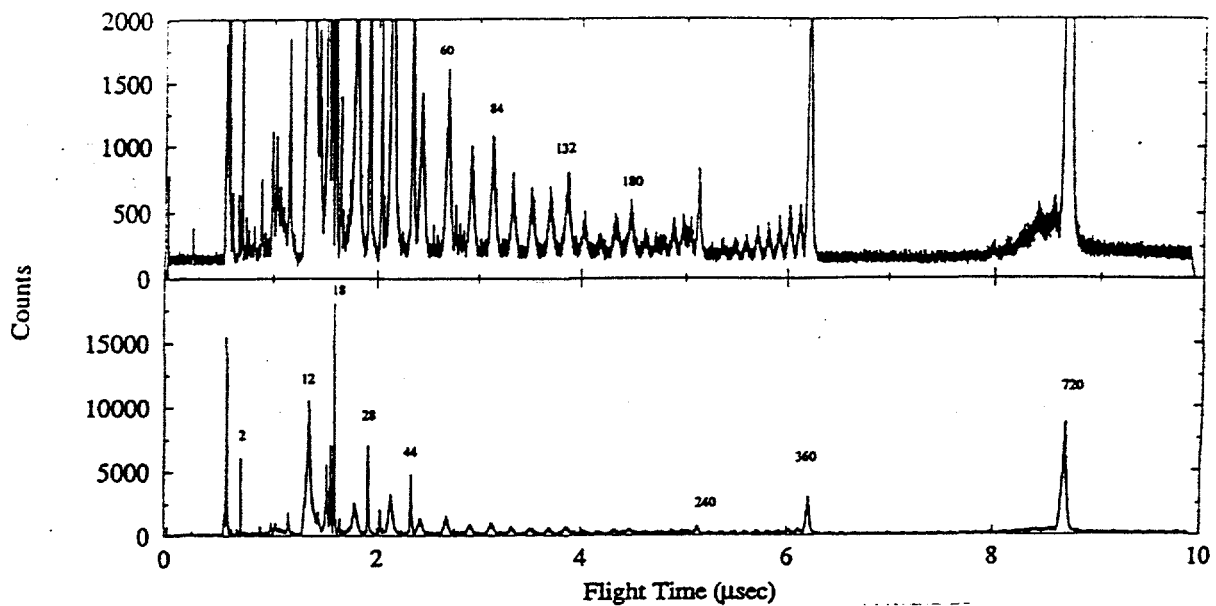


Figure 1. Time-of-flight spectrum for bombardment of C_{60} by 625 MeV $^{136}Xe^{35+}$ ions. The numbers labeling the peaks give the calibration in terms of M/Q , the ratio of fragment mass (amu) to charge.

the accelerator's timing system.

Fig. 1 shows a TOF spectrum for bombardment of C_{60} by 625 MeV $^{136}Xe^{35+}$ ions. The numbers labeling the peaks give the calibration in terms of M/Q , the ratio of fragment mass (in amu) to charge. This spectrum is the sum of all eight channels in the time digitizer and thus reflects all positive fragments detected. Clusters ranging from single carbon atoms up to C_{60}^+ are observed. The TOF spectrum also exhibits peaks attributable to light background gases such as H_2O , N_2 , O_2 , and CO_2 .

The peaks in Fig. 1 that correspond to interactions of the projectiles with C_{60} fall into three categories:

(1) Peaks due to singly, doubly, triply, and (possibly) quadruply ionized C_{60} . These "parent" peaks decrease in relative intensity towards higher charge states. Their narrowness reflects the small kinetic energy releases involved in the generation of these ions.

(2) Even-numbered high mass peaks (ENHM) corresponding to the loss of even numbers of carbon atoms. Interestingly, these ENHM peaks (C_{58}^{q+} , C_{56}^{q+} , C_{54}^{q+} , etc.) are stronger relative to their parent peaks for the higher charge states.

(3) Peaks corresponding to the sequence of singly charged fragments C_n^+ , with n assuming all values from 1 to at least 19 (higher values then become indistinguishable from the multiply charged pair-loss peaks). These peaks alternate in intensity up to around $n=9$ with the odd-numbered peaks being more intense than the even-numbered. Above $n=9$, the most intense peaks appear to be $n = 11, 15$, and probably 19. These intensity variations mirror those seen in other studies^{5,6}. We refer to this series of peaks, C_n^+ as the "multifragmentation" peaks since we believe (see below) that they arise predominantly from events in which there is a catastrophic disintegration of the molecule into many small fragments.

The manner in which energy is coupled into the C_{60} system from the passage of a highly charged fast ion (of velocity v) can be expected to depend strongly on the impact parameter. The two principal distances of importance in discussing impact parameters are the mean radius, R (known² to be 3.55 Å) of the C_{60} "cage" on which are located the nuclei of the constituent carbon atoms, and the adiabatic distance⁷ $b_0 = \gamma \hbar v / E$

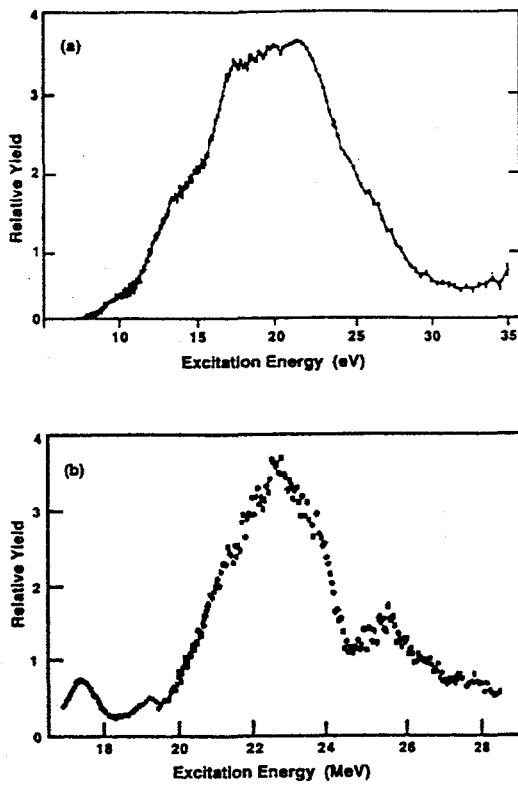


Figure 2. comparison of the giant dipole resonances observed in the C₆₀ molecule⁹ and in the ¹²C nucleus¹¹.

(=10 Å for $E = 20$ eV), for the excitation of the giant dipole plasmon resonance of energy E . This collective excitation of the 240 valence electrons of the C₆₀ molecule has been predicted⁸ and measured^{9,10} to have an energy of 20 eV, and a FWHM of about 10 eV. An interesting connection to nuclear physics is shown in Fig. 2, which gives a comparison of the giant dipole resonances observed in the C₆₀ molecule⁹ and in the ¹²C nucleus¹¹.

To estimate the total interaction cross section, we developed a quasi-classical model for the interaction¹² between the projectile and the fullerene that gives the total excitation and single-plasmon excitation probabilities as a function of impact parameter. These probabilities are presented in Fig 3(a). The total excitation probability reaches unity at an impact parameter of about 7 Å, still far outside the radius R. To determine the total interaction cross section, it is therefore not necessary to consider explicitly reactions at the smaller impact parameters where the xenon ion may interact with individual electrons. Using the model, we find that the total interaction cross section is 811 Å², whereas the single-plasmon cross section is 387 Å², i.e. 48% of the total.

Our model can be expected to be valid for single-plasmon excitation involving large impact parameters where the linear-response and dipole approximations are valid. It can be expected to break down at smaller impact parameters where multi-plasmon excitation occurs leading to multiple ionization, pair emission, and (at still smaller impact parameters) multifragmentation. The dominant decay mode of the single-plasmon excitation is via single electron emission^{9,10,13}. We therefore compare the calculated single-plasmon cross section to our measured C₆₀⁺ yield. The dependence on beam energy is illustrated in Fig. 3(b) for the projectile charge state Z_p = 18. The weak dependence on beam energy is reproduced by the calculation. Rough estimates of the experimental cross sections agree with the calculated values within a factor of two. The slope of the

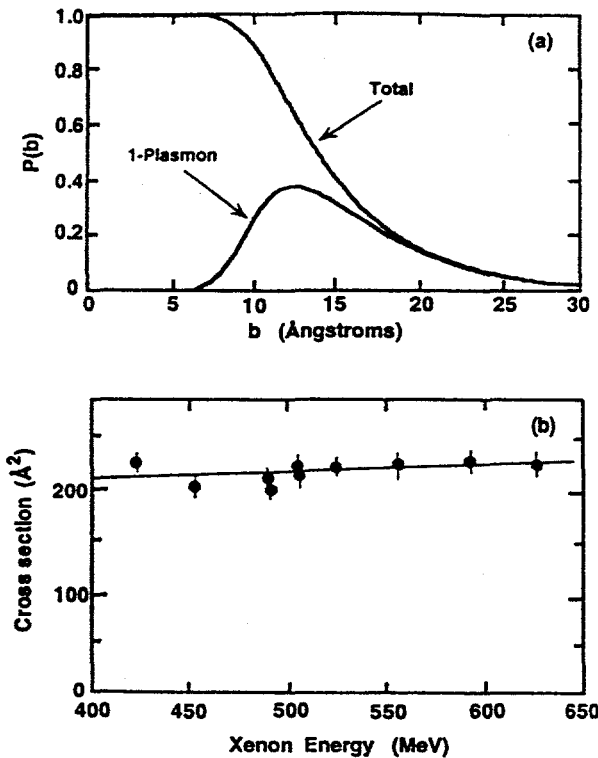


Figure 3. (a) Calculated probabilities for plasmon excitation vs impact parameter. (b) Calculated single-plasmon cross section compared to the measured yield of C_{60}^+ from $\text{C}^{136}\text{Xe}^{18+}$ ions.

calculated curve is insensitive to small variations in the total oscillator strength. We also considered the role of electron capture by the Xe ions as a production mechanism for C_{60}^+ ions but at the high velocities (11-14 a.u.) of our beams, the charge-capture cross sections¹⁴ are negligible compared to the cross sections for plasmon excitation.

At impact parameters less than about 7 Å where the energy deposition becomes large, essentially all projectile/target interactions can be expected to result in multifragmentation. We have constructed a bond-percolation model¹² to describe these fragmentation processes. C_{60} is represented as a collection of lattice sites located at the positions of the carbon atoms. Each site is connected to its three nearest neighbors via bonds. We assume that each xenon ion deposits excitation energy in proportion to its pathlength through the hollow fullerene structure. The energy is then rapidly distributed in a uniform manner over the whole C_{60} -cluster. This leads to the breaking of individual bonds with a probability proportional to the total energy deposition, which in turn, is dependent on the impact parameter.

After computing the breaking of the bonds by a given projectile, we employ a cluster recognition algorithm and identify the sites still connected via unbroken bonds as members of a cluster. We record the size of each cluster. This model is, except for considerations of the different reaction geometries involved, similar to a model of nuclear multi-fragmentation¹⁵⁻¹⁷ used to explain production cross sections¹⁸ for nuclear fragments emerging from heavy nuclei bombarded by protons with energies between 80 and 300 GeV.

Figure 4 shows the fragment-mass distribution calculated using the model. The calculation reproduces the overall shape of the measured fragment-mass spectrum. The calculation gives too little yield at high mass numbers because it does not take into account a) the contributions from evaporative processes following more gentle excita-

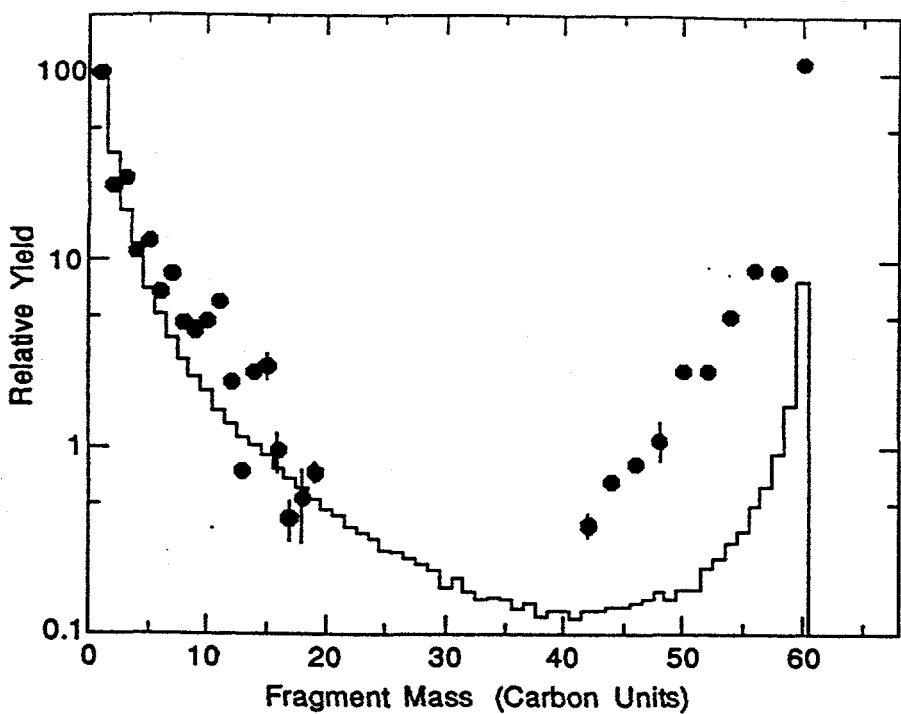


Figure 4. C_{60} bombarded by 625 MeV $^{136}Xe^{35+}$ ions. The histogram is the distribution calculated on the basis of a percolation-multifragmentation model (see text).

tions (eg. plasmon excitations), and b) the known instability of odd-numbered heavy fragments which decay rapidly into even-numbered ones.

Nuclear multifragmentation displays features similar to those observed in our data on fullerene disintegration, eg. the phenomenon of limiting fragmentation (the fragmentation yield does not change much above a certain beam energy). Another common feature is the U-shaped fragment-mass spectrum.

Both experiment and calculation display a power-law fall-off in the production cross sections for clusters of n carbon atoms, $\sigma(C_n) \propto n^{-\lambda}$ for $n \leq 20$. In experiment and calculation, $\lambda \approx 1.3$. This behavior is similar to the case of nuclear fragmentation¹⁸ where one finds $\lambda \approx 2.6$ in inclusive (impact-parameter integrated) reactions. The power law is a consequence of the finiteness of the system and of the integration over different excitation energies in inclusive reactions¹⁵. The nuclear fragmentation data contain indications of a second-order phase transition in nuclear matter (albeit washed out due to finite-size effects), and at the critical point the apparent exponent λ has a minimum^{16,17}. Our λ value is significantly lower than the critical exponent ($\tau=2.0$) for two-dimensional infinite-size bond-percolation and can be attributed to the finiteness and the periodic boundary conditions of our fullerene. Similar observations¹⁹ have been recorded for nuclear systems.

Acknowledgments

This work was supported by the U.S. Department of Energy, Office of Basic Energy Sciences under Contract Nos. W-31-109-ENG-38.

REFERENCES

1. H.W. Kroto, J.R. Heath, S.C. O'Brien, R.F. Curl, and R.E. Smalley, "C₆₀: Buckminsterfullerene," *Nature*. 318:162 (1985).
2. W. Krätschmer, L.D. Lamb, K. Fostiropoulos, and D.R. Huffman, "Solid C₆₀: a new form of carbon," *Nature*. 347:354 (1990).
3. B. Walch, *et al.*, "Electron capture from C₆₀ by slow multiply charged ions," *Phys. Rev. Lett.* 72:1439 (1994).
4. E.E.B. Campbell, *et al.*, Collision experiments with C₆₀⁺, in: "Nuclear physics concepts in atomic cluster physics," R.S. Schmidt, *et al.*, ed., Springer Verlag, Berlin (1992) p. 185.
5. G. von Helden, *et al.*, "Carbon cluster cations with up to 84 atoms: structures, formation mechanism, and reactivity," *J. Phys. Chem.* 97:8182 (1993).
6. V.E. Dörnenburg and H. Hintenberger, "Das Auftreten vielatomiger Kohlenstoffmoleküle im Hochfrequenzfunken zwischen Graphitelektroden," *Z. Naturforsch.* 14A:765 (1959).
7. N. Bohr, "The penetration of atomic particles through matter," *K. Dan. Vidensk. Selsk. Mat.-Fys. Medd.* 18 (1948).
8. G.F. Bertsch, *et al.*, "Collective plasmon excitations in C₆₀ clusters," *Phys. Rev. Lett.* 67:2690 (1991).
9. I.V. Hertel, *et al.*, "Giant plasmon excitation in free C₆₀ and C₇₀ molecules studied by photoionization," *Phys. Rev. Lett.* 68:784 (1992).
10. J.W. Keller and M.A. Coplan, "Electron energy loss spectroscopy of C₆₀," *Chem. Phys. Lett.* 193:89 (1992).
11. R.G. Allas, S.S. Hanna, L. Meyer-Schützmeister, and R.E. Segel, "Radiative capture of protons by B¹¹ and the giant dipole resonance in C¹²," *Nucl. Phys.* 58:122 (1964).
12. T. LeBrun, H.G. Berry, S. Cheng, R.W. Dunford, H. Esbensen, D.S. Gemmell, E.P. Kanter, and W. Bauer, "Ionization and Multifragmentation of C₆₀ by High-Energy, Highly Charged Xe Ions," *Phys. Rev. Lett.* 72:3965 (1994).
13. T. Drewello, W. Krätschmer, M. Fieber-Erdman, and A. Ding, "Photoionization dynamics of C₆₀ studied with synchrotron radiation," *Int. J. Mass Spectrosc. and Ion Proc.* 124:R1 (1993).
14. A.S. Schlachter, *et al.*, "Electron Capture for fast highly charged ions in gas targets: an empirical scaling rule," *Phys. Rev. A*. 27:3372 (1983).
15. W. Bauer, "Extraction of signals of a phase transition from nuclear multifragmentation," *Phys. Rev. C*. 38:1297 (1988).
16. W. Bauer, *et al.*, "The nuclear lattice model of proton-induced multi-fragmentation reactions," *Nucl. Phys.* A452:699 (1986).
17. W. Bauer, *et al.*, "New approach to fragmentation reactions: the nuclear lattice model," *Phys. Lett.* 150B:53 (1985).
18. A. Hirsch, *et al.*, "Experimental results from high energy proton-nucleus interactions, critical phenomena, and the thermal liquid drop model of fragment production," *Phys. Rev. C*. 29:508 (1984).
19. L. Phair, W. Bauer, and C.K. Gelbke, "Percolation with bubbles and toroids," *Phys. Lett.* B314:271 (1993).

DISCLAIMER

This report was prepared as an account of work sponsored by an agency of the United States Government. Neither the United States Government nor any agency thereof, nor any of their employees, makes any warranty, express or implied, or assumes any legal liability or responsibility for the accuracy, completeness, or usefulness of any information, apparatus, product, or process disclosed, or represents that its use would not infringe privately owned rights. Reference herein to any specific commercial product, process, or service by trade name, trademark, manufacturer, or otherwise does not necessarily constitute or imply its endorsement, recommendation, or favoring by the United States Government or any agency thereof. The views and opinions of authors expressed herein do not necessarily state or reflect those of the United States Government or any agency thereof.